Wave-Function Mapping of InAs Quantum Dots by Scanning Tunneling Spectroscopy

Theophilos Maltezopoulos, Arne Bolz, Christian Meyer, Christian Heyn, Wolfgang Hansen,
Markus Morgenstern, and Roland Wiesendanger

Institute of Applied Physics, University of Hamburg, Jungiusstrasse 11, D-20355 Hamburg, Germany

Scanning tunneling spectroscopy is used to investigate the single-electron states and the corresponding squared wave functions of single and freestanding strain-induced InAs quantum dots grown on GaAs(001). Several peaks are found in dI/dV curves, which belong to different single-electron states. Spatially resolved dI/dV images reveal (000), (100), (010), (200), and (300) states, where the numbers describe the number of nodes in $[1\bar{1}0]$, $[110]$, and $[001]$ directions, respectively. The total number and energetic sequence of states is different for different dots. Interestingly, the (010) state is often missing, even when (200) and (300) states are present. We interpret this anisotropy in electronic structure as a consequence of the shape asymmetry of the dots.

     PACS numbers: 73.21.La, 68.65.Hb, 73.22.Dj

Strain-induced InAs quantum dots (QDs) belong to the family of artificial atoms [1]. They exhibit confinement on the nm scale in all three dimensions and atomiclike single-electron states with large energy separations [2–6]. Because of the large energy separation the QDs are interesting for technological applications such as new laser materials [7] or single photon sources [8]. A basic property of the QDs is the wave functions of the confined states. They have previously been probed indirectly by magnetotunneling spectroscopy relying on a transformation of k-space data into real space data [9]. Also cross-sectional scanning tunneling microscopy (STM) images indicate the existence of an s and a p state in the conduction band of a single QD, although the corresponding states have not been identified in dI/dV data [10].

Here, we use low-temperature scanning tunneling spectroscopy (STS) to perform a systematic study of the shape of the squared wave functions $|\Psi_i(x, y)|^2$. We investigate freestanding QDs deposited on GaAs(001) and get full access to the geometrical shape of the QDs, their single-particle peaks in the density of states, and the spatial distribution of the corresponding $|\Psi_i(x, y)|^2$. Surprisingly, we find that the asymmetric shape of the freestanding QDs strongly lifts the degeneracy of the (100) and the (010) states. This partly leads to the appearance of (200) and (300) states in the absence of a (010) state, which should be considered for the interpretation of other physical properties of QDs [11].

The strain-induced InAs QDs are grown by molecular beam epitaxy (MBE) at a base pressure below 4×10^{-11} mbar. N-doped GaAs(001) ($N_D \simeq 2 \times 10^{18}$ cm^{-3}) is first overgrown with an n-doped buffer layer ($N_D \simeq 2 \times 10^{18}$ cm^{-3}) of 400 nm thickness at $T = 600\,°C$ followed by an undoped tunneling barrier of 15 nm thickness ($N_A < 10^{15}$ cm^{-3}). Then, 2.0 ML of InAs are deposited at 495 °C in order to form the QDs. These growth parameters are found to be suitable to create relatively high QDs with a large number of confined states. The samples are transferred from the MBE system to the STM within

1 h by a mobile UHV transfer system at $p < 10^{-9}$ mbar. Only this *in vacuo* transfer allowed us to obtain highly reproducible dI/dV curves.

The STM operates at $p \ll 10^{-10}$ mbar and $T = 6$ K with a maximum energy resolution of $\delta E = 2$ meV [12]. STM images are recorded in constant-current mode using W and PtIr tips. The differential conductivity $dI/dV(V, x, y) \propto \text{LDOS}(eV, x, y) = \sum_{\delta E} |\Psi_i(E_i, x, y)|^2$ [13] is recorded by a lock-in technique ($V_{\text{mod}} \simeq 20$ mV). Therefore, the tip-surface distance is stabilized at each point (x, y) (typically 150×150 points) at voltage V_{stab} and current I_{stab}. Then, the feedback is switched off and a dI/dV curve is recorded from V_{start} to V_{end} ($V_{\text{start}} \leq V_{\text{stab}}$). A sequence of 64 dI/dV images corresponding to different values of V_{sample} results. If δE is smaller than the energy separation between confined states, a single $|\Psi_i(E_i, x, y)|^2$ is displayed in a single dI/dV image.

Figure 1(a) shows the sample geometry. The tunnel barrier decouples the states of the QDs from the degenerately doped backgate. The STM tip and the path of the tunneling current (I) are marked. The band profile along the I path is displayed in Fig. 1(b) as estimated with a 1D-Poisson solver neglecting the influence of the 3D confinement [14]. As parameters we use a QD height of $H = 9.4$ nm, a tip work function of 5.3 eV (PtIr), and a conduction band offset between QDs and GaAs of 390 meV according to 40% Ga content within the QDs [15]. The voltage V_{sample} is adapted to tunnel into a quantized state of the QD. Note the lever arm, i.e., V_{sample} is much larger than the energy of the quantized state with respect to the QD conduction band minimum.

Figure 1(c) shows a constant-current image of the QD sample. Besides the bright QDs, several steps are visible on the wetting layer (WL). Most QDs have a lateral extension of 21 ± 2 nm along $[1\bar{1}0]$ and 16 ± 2 nm along $[110]$. Only one dot in the lower right area is considerably larger (60×40 nm^2). Such dots are regularly found on the sample, but do not show any spectral features in STS. A 3D representation of a typical QD is shown in the left
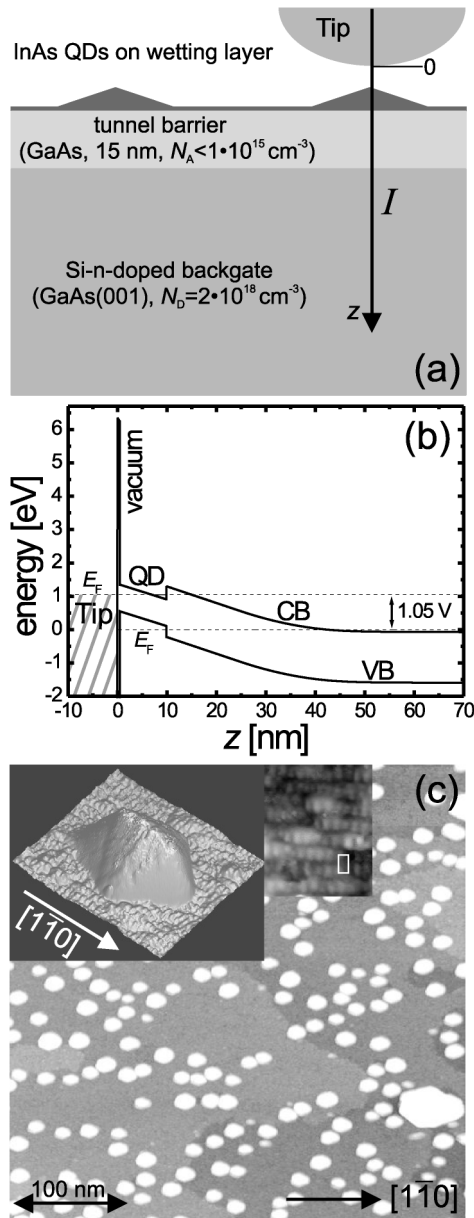
FIG. 1. (a) Sketch of STS measurement of the sample with freestanding InAs QDs; tunneling path I along z is indicated; (b) band profile along the z direction marked in (a) as calculated with a 1D-Poisson solver [14], $V_{sample} = 1.05$ V, CB: conduction band, VB: valence band; a confined QD state is marked as a full black line; (c) constant-current image of the InAs-QD sample, $V_{sample} = 3$ V, $I = 70$ pA; left inset: 3D representation of a typical QD with the $[1\bar{1}0]$ direction marked; central inset: wetting layer with atomic resolution; (2×4) unit cell (white rectangle) is marked.

inset being comparable to previous STM results [16]. As all QDs, the QD is more extended in the $[1\bar{1}0]$ direction, thus, we observe a shape asymmetry. Note the superstructure on the WL shown in the central inset, which is compatible with a disordered (2×4) reconstruction.

A constant-current image of a single, relatively small QD is shown in Fig. 2(a). Figure 2(b) shows the corresponding $I(V)$ curve recorded above the QD (black line)

in comparison with an $I(V)$ curve recorded on the WL (grey line). While only a continuous $I(V)$ increase appears on the WL [17], two current steps are observed on the QD. In the simultaneously recorded dI/dV curves [Fig. 2(c)], the two steps appear as two peaks with full width at half maximum (FWHM) of 70 and 150 meV. The peaks are caused by the two quantized states of the QD. In order to prove that we investigate the peak intensity as a function of position. The dI/dV curves of Fig. 2(d) reveal that the intensity of the first peak decreases with distance from the QD center, while the intensity of the second one increases. In addition, the whole spectrum shifts to higher energies. The latter is probably caused by the increased band bending at a smaller distance between the tip and the degenerately doped GaAs backgate, if the tip is at the rim of the QD. However, since the resulting peak shifts are small, dI/dV images still largely represent the peak intensity as a function of position. Figure 2(e) shows the dI/dV image recorded at the first peak of Fig. 2(c), while Fig. 2(f) shows the dI/dV image at the second peak. Obviously, the first peak has a circular symmetric intensity distribution as expected for a (000) state, while the second one has a pronounced node in the center as expected for a (100) state [3,4]. The measured patterns obviously correspond to the shape of the squared wave functions of individual states.

The width of the peaks in Fig. 2(c) requires some discussion. It is basically given by the lifetime of the electrons in the confined states. An upper boundary for this lifetime is the tunneling rate r through the undoped GaAs tunnel barrier. It can be estimated according to the method described in [18]. Therefore, the band bending within the sample has to be taken into account. The resulting triangular tunnel barrier behind the QD is visible in Fig. 1(b). Depending on the confinement energy of the state, we find $10^{12}/s \leq r \leq 3 \times 10^{13}/s$. This is much larger than typical tunneling rates from the tip to the QD ($r \simeq 3 \times 10^8/s$). Accordingly, the intrinsic lifetime broadening of the QD states should be up to about 20 meV. Considering the average lever arm factor in our experiment of about 5.5, which is deduced straightforwardly from the 1D-Poisson calculations, we expect single-particle peaks with FWHM up to about 110 meV. As in Fig. 2(c), we partly find larger FWHMs by up to a factor of 2 [19], which we attribute to simplifications within the estimate.

To get statistically relevant information on the state sequences and to prove the reliability of the method, we investigated 25 different QDs deposited on three different samples. The results on three further QDs, all exhibiting more than two states, are shown in Fig. 3. Again, the QDs appear elongated in the $[1\bar{1}0]$ direction as shown in Figs. 3(a1), 3(b1), and 3(c1). The dI/dV curves in Figs. 3(a2), 3(b2), and 3(c2) are spatially averaged over the whole QD area. Because of the discussed peak shift as a function of position, the peaks are less well resolved. But since we map the squared wave functions, we can
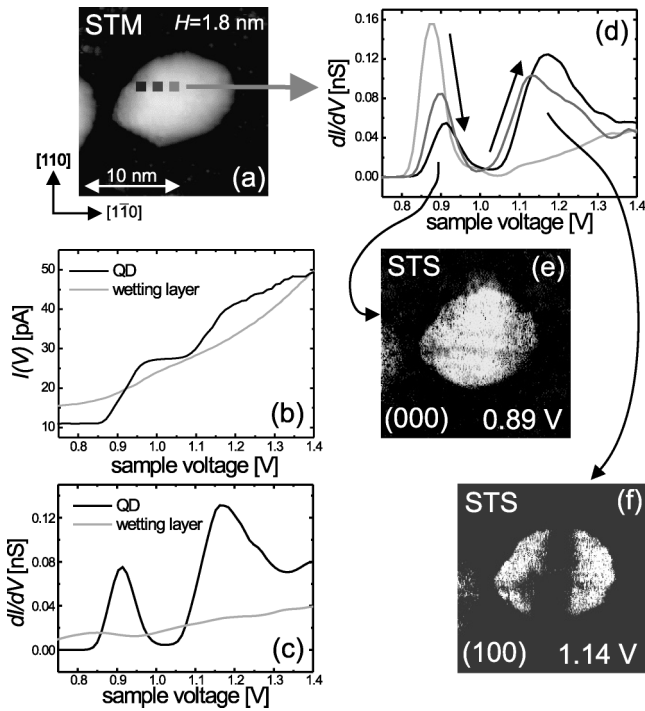
FIG. 2. Single QD, W tip: (a) constant-current image, $V_{sample} = 1.7$ V, $I = 50$ pA, height H and crystallographic directions marked; (b) $I(V)$ curves recorded on the QD (black line) and on the wetting layer (grey line), $V_{stab} = 1.6$ V, $I_{stab} = 50$ pA; (c) dI/dV curves recorded simultaneously with (b), $V_{mod} = 28$ mV; (d) dI/dV curves recorded at different positions above the QD as marked in (a); (e),(f) spatially resolved dI/dV data at $V_{sample} = 0.89$ V and $V_{sample} = 1.14$ V, respectively; all data in Fig. 2 are raw data.

easily attribute the peaklike features to different states. Therefore, we inspect all 64 dI/dV images for each QD and find only the symmetries presented in Fig. 3 which indeed correspond to the peaklike features. The state sequences are (000), (100), and (200) for Figs. 3(a3), 3(a4), and 3(a5) (left row); (000), (100), (010), and (200) for Figs. 3(b3), 3(b4), 3(b5), and 3(b6) (middle row); and (000), (100), (200), and (300) for Figs. 3(c3), 3(c4), 3(c5), and 3(c6) (right row). For comparison, calculated squared wave functions are shown on the left of Fig. 3 (from [3]).

Table I summarizes the state sequences found for 25 different QDs with heights between 1.7 and 9.4 nm (mean value: 4.5 nm). 40% of the QDs exhibit only a (000) state, but up to four states are partly observed. Generally, we find that higher dots exhibit more states. Most surprisingly, (200) and (300) states partly appear without the appearance of a (010) state. Thus, we find a strong anisotropy in the electronic structure. To emphasize that, we sum up all nodes in the $[1\bar{1}0]$ and $[110]$ directions for the 25 QDs and get 33 and 3 nodes, respectively.

The found electronic anisotropy could be caused by the shape asymmetry of the QDs. An average aspect ratio of $A = 1.3$ is found in the STM image of Fig. 1(c). Partly larger aspect ratios appear in Fig. 3: $A = 1.6$ for
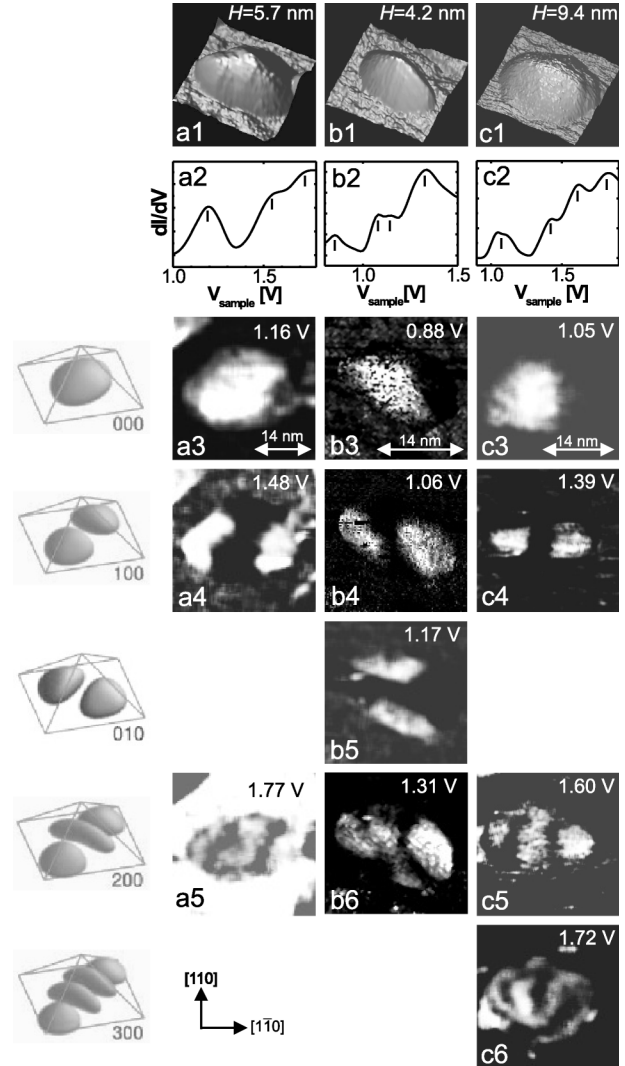

FIG. 3. STS data of three different QDs: (a1)–(c1): 3D representation of constant-current images with heights H indicated; (a2),(b2),(c2): $dI/dV(V)$ curves spatially averaged over the QD area, peak positions are marked by vertical lines; (a3)–(a5), (b3)–(b6), (c3)–(c6): dI/dV images recorded at V_{sample} as indicated; data are partly smoothed in order to enhance picture quality; the state in (a5) exhibits an energy close to the onset of the wetting layer, which results in a bright surrounding of the wave function; crystallographic directions are marked; (a1)–(a5): W tip, $V_{stab} = 1.85$ V, $I_{stab} = 50$ pA, $V_{mod} = 15$ mV; (b1)–(b6): W tip, $V_{stab} = 1.6$ V, $I_{stab} = 50$ pA, $V_{mod} = 27$ mV; (c1)–(c6): PtIr tip, $V_{stab} = 2.4$ V, $I_{stab} = 70$ pA, $V_{mod} = 15$ mV; constant-current images at $V_{sample} = V_{stab}$ and $I = I_{stab}$; left column: calculated squared wave functions taken from [3] and labeled by the number of nodes in different directions.

Figs. 3(a1) and 3(b1) and $A = 1.4$ for 3(c1). These relatively large aspect ratios lead to a much stronger confinement in $[110]$ than in the $[1\bar{1}0]$ direction. Taking the different base plane lengths of the QDs in Fig. 3 as the input parameter for published theoretical calculations of the QD state energies [3,4], we find that the confinement energy for the (010) state should be 100 meV higher than the (100) state. To compare this with experiment, we have

TABLE I.　Energetic state sequence for 25 different QDs.

State sequence	Number of QDs
(000)	10
(000), (100)	7
(000), (100), (010)	2
(000), (100), (010), (200)	1
(000), (100), (200)	3
(000), (100), (200), (300)	2

to translate the measured peak voltages V_{sample} into energies E by using the 1D-Poisson solver [14]. For the states of Figs. 3(c3), 3(c4), 3(c5), and 3(c6) at $V_{sample} = 1.05, 1.39, 1.60,$ and 1.72 V we find $E = 139, 212, 254,$ and 278 meV with respect to the conduction band minimum of the QD. Accordingly, the (010) state should appear around $(212 + 100 = 312)$ meV, which is indeed above the energy of the (300) state. Thus, we can explain the state sequence qualitatively. However, the shape asymmetry cannot explain all details. For example, the shape asymmetry in Fig. 3(b1) is larger than in 3(c1), although the (010) state is found only in the former case [20]. Thus, detailed calculations taking the shape and the stress fields of the QDs into account are highly desirable.

Note finally that the strong electronic anisotropy found by STS is not found by capacitance measurements [6], far-infrared measurements [5], or magnetotunneling experiments [21], all performed on capped QDs. The magnetotunneling reveals rather degenerate (010) and (100) states, while the other methods imply an energy difference of 2–10 meV between the levels. This difference is tentatively explained by shape asymmetry as well as by exchange effects. Importantly, none of the authors of [5,6,21] find an indication for a (200) state appearing prior to the (010) state. The most likely explanation is that the QD shape changes during overgrowth.

In summary, we mapped the squared wave functions of single and freestanding strain-induced InAs QDs grown on GaAs(001). The QDs show one to four single-electron states which are identified as (000), (100), (010), (200), and (300) states. The numbers are the number of nodes in the $[1\bar{1}0]$, $[110]$, and $[001]$ directions, respectively. Different energy sequences of states are found for different QDs, but states with nodes in the $[1\bar{1}0]$ direction appear much more often than states with nodes in the $[110]$ direction. This strong electronic anisotropy is largely attributed to the shape asymmetry of the QDs.

[1] D. Bimberg et al., Quantum Dot Heterostructures (Wiley, New York, 1999).
[2] H. Jiang et al., Phys. Rev. B 56, 4696 (1997).
[3] O. Stier et al., Phys. Rev. B 59, 5688 (1999).
[4] M. Grundmann et al., Phys. Rev. B 52, 11 969 (1995); A. J. Williamson et al., Phys. Rev. B 59, 15 819 (1999); L. C. R. Fonseca et al., Phys. Rev. B 57, 4017 (1998); C. Pryor, Phys. Rev. B 60, 2869 (1999).
[5] M. Fricke et al., Europhys. Lett. 36, 197 (1996).
[6] B. T. Miller et al., Phys. Rev. B 56, 6764 (1997); R. J. Luyken et al., Appl. Phys. Lett. 74, 2486 (1999).
[7] Y. Qiu et al., Appl. Phys. Lett. 79, 3570 (2001).
[8] P. Michler et al., Science 290, 2282 (2000); Z. Yuan et al., Science 295, 102 (2002).
[9] E. E. Vdovin et al., Science 290, 122 (2000); M. Narihiro et al., Appl. Phys. Lett. 70, 105 (1997).
[10] B. Grandidier et al., Phys. Rev. Lett. 85, 1068 (2000).
[11] See, e.g., G. W. Bryant, Appl. Phys. Lett. 72, 768 (1998); J. Shumway et al., Phys. Rev. B, 63, 155316 (2001).
[12] Chr. Wittneven et al., Rev. Sci. Instrum. 68, 3806 (1997).
[13] J. Tersoff et al., Phys. Rev. B 31, 805 (1985); M. Morgenstern et al., J. Electron Spectrosc. Relat. Phenom. 109, 127 (2000).
[14] G. L. Snider et al., J. Appl. Phys. 68, 2849 (1990).
[15] Grazing incidence x-ray diffraction on an identically grown sample performed according to the method described by I. Kegel et al. [Phys. Rev. Lett. 85, 1694 (2000)] indicates an average Ga content of 33% increasing towards the bottom of the QD; A. Bolz et al., HASYLAB Ann. Rep. 1, 733 (2002).
[16] Y. Hasegawa et al., Appl. Phys. Lett. 72, 2265 (1998); J. Márquez et al., Appl. Phys. Lett. 78, 2309 (2001); G. Costantini et al., Appl. Phys. Lett. 82, 3194 (2003).
[17] We interpret the $I(V)$ increase on the WL as due to a direct tunneling of electrons from the tip to the degenerately doped GaAs.
[18] C. M. A. Kapteyn et al., Phys. Rev. B 60, 14 265 (1999).
[19] We checked that the FWHM does not decrease with decreasing V_{mod}.
[20] From previous experiments [Dombrowski et al., Phys. Rev. B 59, 8043 (1999)], we know that the tip induced electric field typically has a FWHM of about 50 nm, which is significantly larger than the extension of the InAs QDs (20 nm). Thus, we believe that a possible asymmetric electric field from the tip is of minor importance for the found electronic anisotropy. Moreover, we found the same anisotropy for about ten individually prepared tips. It is rather unlikely that all these tips have a shape asymmetry along the $[1\bar{1}0]$ direction of the sample.
[21] A. Patané et al., Phys. Rev. B 65, 165308 (2002); an electronic anisotropy is, however, found for QDs grown on GaAs(113)B.